Planar Metasurface External Cloak

Yineng Liu[†, ‡], Jinying Xu[§], Shiyi Xiao[†], Xianzhong Chen[3] and Jensen Li[†,*]

[†] *School of Physics and Astronomy, University of Birmingham, Birmingham B15 2TT, United Kingdom*

[‡] *Institute of Electromagnetics and Acoustics and Department of Electronic Science, Xiamen University, Xiamen 361005, China* [§]*Department of Physics, Fuzhou University, Fuzhou 350108, Fujian, China*

[3]*SUPA, Institute of Photonics and Quantum Sciences, School of Engineering and Physical Sciences, Heriot-Watt University, Edinburgh, EH14 4AS, U.K.*

ABSTRACT

Metasurface, with only single layer of artificial atoms for ease of fabrication, can become a practical surface-equivalent route to transformation optical (TO) applications. The previous design paradigm for a metasurface carpet cloak is based on straight-forward phase compensation, hampering more general wave manipulations. Here, we propose a theoretical approach in designing metasurface using the concept of complementary media as an intermediate step. The metasurface, effectively storing all the original information in TO media, enables specific TO applications which normally requires complementary media. A passive external metasurface cloak is numerically demonstrated here, which can hide an object on top of a reflective metasurface, mimicking a flat mirror. Furthermore, our scheme enables metasurfaces to be used to construct arbitrary standing waves on-demand, which will be useful for constructing tailor-made cavity modes, optical trapping and illusion-type TO applications, which can project holograms in addition to scattering cancellation.

KEYWORDS: metasurface, external cloak, transformation optics, artificial electromagnetic boundary, complementary media, scattering control

Metasurfaces, consisting of only a limited number of layers of metamaterial atoms, are capable to manipulate wavefront with subwavelength resolution. These materials allow demonstrations of a variety of unique and interesting phenomena and applications, such as anomalous refraction/reflection [1-5], ultrathin flat lenses [6,7], surface-enabled vortex beams manipulation [8,9], and holograms with high efficiency [10-12]. Comparing to bulk form of metamaterials, such a surface approach of metamaterials also paves a way to have easier fabrication, to increase operational bandwidths and to keep absorption losses to manageable amount [3,5]. Keeping in mind that one of the promising application for metamaterials is invisibility or transformation optics (TO) in a more general context [13-18], metasurfaces have been recently experimentally demonstrated as ultrathin skin cloaks in both optical and microwave regime [19-23]. Such a cloak is essentially accomplished by a tailor-made reflection phase profile from the metasurface to compensate the missing phase elapse of a curved region. More importantly, by extending the metasurfaces to include active gain components, more generic transformation optical applications have been proposed by constructing reflective metasurfaces with complex surface susceptibility[24]. For example, a flat surface can be made to reflect like an arbitrarily curved surface [24]. However, for more generic types of illusion applications, negative index or complementary media are often required, e.g. to construct an external cloak or give an illusion of change of object[25,26]. In these cases, a mere consideration of phase compensation from a boundary with complex surface susceptibility is not enough for generic applications and for practical implementations. In this letter, by combining two seemingly different approaches: one on retrieving the surface impedances from desired wave discontinuities [27-29] and another on transformation optics with complementary media [25,26] we

present a unique approach to construct a planar metasurface cloak that can hide an object that is external to the metasurface cloak itself. It thus works like the surface version of the TO external cloak. Furthermore, based on the same principle, metasurfaces are also constructed to hold arbitrary designer cavity modes, which will be useful in the applications involving manipulation of cavity modes, such as optical trapping and sensing[30-33].

DESIGN OF PLANAR METASURFACE EXTERNAL CLOAK

The schematic diagram illustrating the design approach of planar metasurface external cloak is shown in Fig. 1. The virtual space (Fig. 1(a)), in TO terminology, is the configuration we would like the observer to perceive. It is just the free-space with a PEC mirror (schematically represented by a black thick line). We assume two-dimensional wave propagation on the $x-y$ plane. The black arrows indicate the incident fields: electric field $E_{in}(r)$ and magnetic field $H_{in}(r)$, and the reflected fields: electric field $E_r(\boldsymbol{r})$ and magnetic field $H_r(r)$, from a flat PEC mirror. On the other hand, the physical space, in the terminology of TO, which contains the physical object to be hidden, is shown in Fig. 1(b). The same incident light ($E_{in}(r)$ and $H_{in}(r)$) impinges on the "real" object (schematically represented by the blue bump with permittivity ε_1 and permeability μ_1) and a metasurface (the dashed line in green colour) to be designed. In order to achieve invisibility, the metasurface has to cancel the scattered field from the "real" object and to generate the target specular reflection $E_r(r)$ from a flat PEC mirror, which should be perceived to appear at the same location of the metasurface, so that an observer outside a certain illusion boundary (the gray dotted line above the object) perceives the situation in Fig. 1(a). One effective way to obtain such an

illusion is through transformation optics with complementary media[25, 26]. Here, we would like to investigate the usage of metasurface to replace the complementary medium so that only a single metasurface is needed instead of bulk negative-index metamaterials for the ease of fabrication. However, as we shall see, the principle behind the complementary media route is actually embedded in the design process of the metasurface.

Our approach has three steps in total. The first step is to simulate the virtual configuration and evaluate the total field $E = E_{in} + E_r$, $H = H_{in} + H_r$ at a fictitious boundary FB1, situated at the location of the gray dotted line (called the illusion boundary) in Fig. 1(a) (or the blue line in Fig. 1(c)). At this stage, we can put a reflecting metasurface at boundary FB1 to replace the flat PEC mirror. A reflecting metasurface, without going into the detailed metamaterial structure in this work, is modelled by a homogenized boundary condition using the surface admittance matrix Y as

$$\begin{pmatrix} -H_x \\ H_z \end{pmatrix} = Y \begin{pmatrix} E_z \\ E_x \end{pmatrix} = \begin{pmatrix} Y_{TE} & \\ & Y_{TM} \end{pmatrix} \begin{pmatrix} E_z \\ E_x \end{pmatrix}. \tag{1}$$

The admittance matrix has zero off-diagonal elements with the assumption that the metasurface does not couple transverse electric (*TE*, with electric field along z) and transverse magnetic (*TM*, with magnetic field along z) polarizations. The required admittance values are then evaluated using the sampled total field at boundary FB1 as

$$\begin{aligned} Y_{TE} &= -H_x / E_z , \\ Y_{TM} &= H_z / E_x . \end{aligned} \tag{2}$$

The metasurface, serving as an artificial electromagnetic boundary in modifying the boundary

FB1 condition, can be also fully described by its reflection phase at normal incidence as the effective 'constitutive parameters'.

$$Y_{TE} = -i \cdot \tan\left(\frac{\varphi_z}{2}\right),$$

$$Y_{TM} = -i \cdot \tan\left(\frac{\varphi_x}{2}\right), \tag{3}$$

where φ_z or φ_x is the reflection phase defined in terms of the *E*-field for TE and TM polarizations. In the second step, we flip the boundary FB1 to boundary FB2 below the PEC through a "mirror" operation using a complementary medium, as shown in Fig. 1(d), and request the field profile outside FB1 being unchanged. The boundary FB1 becomes simple continuity while the boundary FB2 becomes a metasurface with appropriate boundary condition. The complementary medium does a one-to-one mapping $(x, y) \leftrightarrow (x, -y)$ between boundary FB1 and FB2. It ensures a corresponding one-to-one mapping on the fields by $(E_x, E_y, E_z) \leftrightarrow (E_x, -E_y, E_z)$ and $(H_x, H_y, H_z) \leftrightarrow (H_x, -H_y, H_z)$. They are just flipped in the y component. As a result, the required admittance values at FB2 are just the same Y_{TE} and Y_{TM} as their mirrored locations. The complementary medium is chosen as the one that the upper half is the target physical configuration (the blue bump and white rectangle area) and the lower half is chosen as its complementary mirrored copy with permittivity $\varepsilon(x, y) = -\varepsilon(x, -y)$ and permeability $\mu(x, y) = -\mu(x, -y)$ in annihilating the upper half. Thus, the total field can be formally transferred, with the presence of the object, step by step downwards up to the location of the target reflecting metasurface. This step is like a seed simulation from TO external cloak to inspire us to design the metasurface version. Instead of

using a transfer matrix formulation to achieve this, here we use a complementary medium, which acts as a numerical way to find the tranfer matrix. Then, full-wave simulation is again performed for this configuration. We now have a configuration that its upper half is the same as the target physical system while the fields outside boundary FB1 is the same as the field in the virtual system. In the final step, we sample the fields in the previous simulation on the location of the target reflecting metasurface, shown in Fig. 1(b)) and obtain its required admittance values according to Eq. (2) and calculate the reflecting phase for the designed planar metasurface through Eq. (3). Now, we have a reflecting metasurface, physical object on top of it and the fields outside FB1 is expected to be the same in the virtual system.

RESULTS AND DISCUSSION

In the following, we apply the above scheme to design a planar metasurface external cloak to conceal a dielectric semi-cylinder at position $(0,0)$, with ε_1=1, μ_1=3 and radius =0.8 in the unit of free-space wavelength λ (set as value one without losing generality). In this case, the virtual space is just the free-space with a PEC mirror, as shown in Fig. 2(a). Here, we take the incident plane wave to have *TE* polarization and an 0^0 incident angle for illustration. Figure 2(c) shows the simulated reflected field profile (we only show the reflected field for clarity: total field minus the incident plane wave) when we have a metamsurface at FB1 (the green line), which ranges from $x=-3$ to 3 and have a height of 1.2. The admittance Y_{TE} is evaluated according to Eq. (2) with the field profile in the virtual space. As shown in the figure, it reproduces the same field in the virtual space outside FB1. Up to

this stage, it corresponds to the ultrathin metasurface cloak in hiding object beneath the metasurface[19-23]. Next, we flip the admittance values on FB1 (the grey dotted line, its position is equivalent to the green line in Fig. 2(c)) by a mirroring action in the y-direction to FB2 in Fig. 2(d). The region in between FB1 and FB2 becomes the physical object (the mentioned dielectric semi-cylinder in air) in the part $y>0$ and its complementary mirrored copy: a cylinder with $\varepsilon_1(x,-y)=-1$, $\mu_1(x,-y)=-3$ and with the same diameter in a negative-index background of $\varepsilon_0(x,-y)=\mu_0(x,-y)=-1$. With such a mirrored metasurface and complementary medium, we perform the simulation again and the reflected field profile is shown in Fig. 2(d). Again, the field profile outside FB1 is the same is the target field profile in the virtual space. From the field profile of this simulation, we can finally obtain the admittance at our target metasurface through Eq. (2) and calculate the reflecting phase for the desiged planar metasurface (Fig. 2(f)). In general, the surface admittance is complex and its real part corresponds to gain or loss. However, it is rigorously a pure imaginary in the following two scenarios: 1. when the electric field is at normal incidence, the total electric field has its electric field being purely real and magnetic field being purely imaginary so that their ratio is a purely imaginary number according to equation (2); or 2. when the target is a cavity field, i.e. a standing wave in the system, with real permittivity and permeability, the surface admittance is again pure imaginary. So for our normal incidence case, a passive (lossless) metasurface with $Y_M=imag(Y_0)\cdot i$ is an accurate description of the ideal surface admittance condition. Here, our approach essentially replaces the external cloak devices originally using bulk negative-index metamaterials by the passive measurface which is below the physical dielectric semi-cylinder. The simulated reflected field from the external

metasurface cloak is shown in Fig. 1(b). With the help of metasurface, the total reflected pattern outside the illusion boundary appears as if there is only a flat PEC boundary as in Fig. 2(a) without observing scattering from the "real" object. Figure 2(e) shows the case when we have only a PEC mirror instead of the metasurface beneath the dielectric semi-cylinder, in which severe scattering happens in contrast.

It is worth to mention that our metasurface is designed ideally for a fixed angle, in order to obtain the required admittance or reflecting phase from the interference between the incident and the reflected waves. It is a general feature for metasurface-enabled cloaking devices [34-38]. Such effect can be regarded as the cost by compressing a bulk device such as carpet cloak to an optically ultra-thin surface. An optically thin device has limited control on angular behaviour, which can only be completely fulfilled if we go to the thick limit. On the other hand, although the metasurface device is only designed for a particular angle, if the target is a cavity field, i.e. a standing wave in the system or the metasurface has a small activeness, some tolerance in the incident angle is expected.

Figure 3(b) and (c) show the case for the same demonstrated external cloak but at an angle of 0^0 or 20^0. In this case, the design working angle is at $10°$ (required reflection phase shown in Fig. 3(a)). They still almost resume the specular reflection from a seemingly flat PEC mirror. For oblique incidence, the admittance profile is now generally complex. We have only taken the imaginary part ($iIm(Y)$, labelled as P.M.) of the designed admittance profile as an approximation. The full active case (labelled as A.M.) is shown in Fig. 3(d) without such an approximation, that obviously reproduces perfect invisibility effect as expected. Our simulation results show that the ideal metasurface can be active and work for oblique incident

wave. But for practical realization, the ideal metasurface can be designed to a passive case (without gain/loss) when the target is a cavity field, i.e. a standing wave in the system.

In addition to more general illusion-type TO applications, the passive metasurface also enables potential applications such as optical trapping and constructing designer cavity modes, etc. It is well known that two relative incident coherent Gauss beams can form Gauss standing wave for the enhancement of optical trapping, but in practical operation, in order to simplify the modulation of optical path, the standing wave is obtained under a microscope objective by the interference of an incoming laser beam and a beam reflected on a microscope slide that has been coated with a system of reflective dielectric layers [30]. On the other hand, the recent development of metasurfaces provide us with an unprecedented opportunity to design the wavefronts of light at will, such as anomalous reflection/refraction and beam focusing with subwavelength resolution[1-9], and may allow us to design tailor-made cavity modes, i.e. a standing wave in the system with the advantage of being more compact and easier for device integration. Here, we would like to investigate the usage of planar metasurface to replace reflective dielectric layers so that only a single passive metasurface and an incoming laser beam can create perfect Gauss standing waves, without focusing effect as well. For illustration, here we target to generate a standing wave from two counter propagating Gaussian beams by using a metasurface, which cuts through the cross section of the two beams at an arbitrary angle (chosen as $45°$ in this example). The beam waist is set as 1.25λ located at origin. Figure 4(a) shows the target E_z-profile from two counter propagating Gauss beams, from which the admittance profile (Fig. 4(b)) by applying Eq. (2) at the location of the metasurface ($y = -3$). Figure 4(c) shows the simulated results, reproducing the target fields,

but now with the metasurface. As the target field is a standing wave, the metasurface is therefore rigorously lossless and passive. The metasurface can actually be put at any angles. It may give rise to additional flexibility and yield more compact designs of optical systems requiring multiple coherent input beams.

Now, we generalize the above principle to construct tailor-made standing waves in cavities. In normal dielectric cavities with a rotational symmetry, whispering gallery modes (WGMs) can be formed by total internal reflection of light around the rim of the cavities. The ultrahigh Q factor of WGMs has enabled a variety of impressive photonic systems, such as microlasers, biosensors and cavity optomechanical devices. Recent research showed the mode properties of two-dimensional dielectric whispering gallery cavities, such as the Q factor and emission directionality, can be tailored using transformation optics and metamaterials [32]. However, previous design methods of WGMs are cumbersome by the boundary element method[32,**Error! Bookmark not defined.**]. Here, our approach provides a straight-forward way for such a purpose. Instead of starting from a physical cavity, we start with the desired profile of the cavity mode and enclose it with metasurfaces to construct the mode. For illustration, we target to construct a WGM mode: $E_z = J_m(kr)e^{jm\varphi} + J_{-m}(kr)e^{-jm\varphi}$ in cylindrical coordinate (r,φ) with J_m being the Bessel function of integer order m. The metasurface, enclosing the mode, is rigorously lossless since E_z is purely real as a standing wave (Fig. 5). Now, we do not need any dielectric media within the cavity to construct the WGM mode. We also leave a small gap at the top of cavity for excitation purpose from a plane wave impinging from the top. Fig. 5 (a), (b) show the results of our simulations of WGMs with order $m = 8$, and 15 respectively. Our simulation results show that the desired passive metasurfaces work very

well. In addition to WGMS, our scheme also enables other desired cavity modes by passive metasufaces.

CONCLUSIONS

In summary, based on combining surface impedance approach and transformation optics approach with complementary media as a seed simulation, we design a metasurface version of transformation optics external cloak. It can hide an object on top of a reflective metasurface, mimicking a flat mirror. This is similar to a TO-based external cloak by using negative index medium to cancel out scattering field of the object but now the metasurface replaces the negative index medium in TO-based external cloak. This is also different from the metasurface skin cloak and carpet cloak, in which the hidden object is beneath the curved metasurface cloak. According to the established design scheme, we demonstrate planar external cloaking metasurface with very good performance. Although our metasurfaces are only designed for a particular predefined incident angle, they can still have angle tolerances about ±10°. Furthermore, the passive metasurface also enables potential applications such as optical trapping and constructing desired cavity modes. Our scheme for metasurface external cloak opens a gate for realizing more complicated transformation optic device with metasurface.

FIGURES

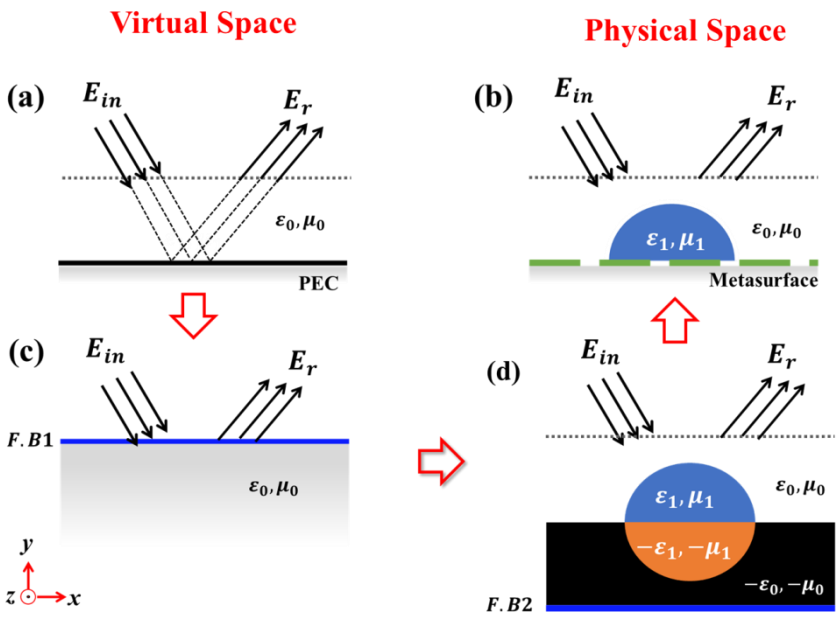

Figure 1. (color online). The schematic diagrams of planar metasurface external cloak. (a) The virtual space with a flat PEC. (b) The physical space with the "real" object to turn into invisibility by metasurface. (c) and (d) are the two auxiliary "virtual" spaces to obtain the design of metasurface in 3 successive steps.

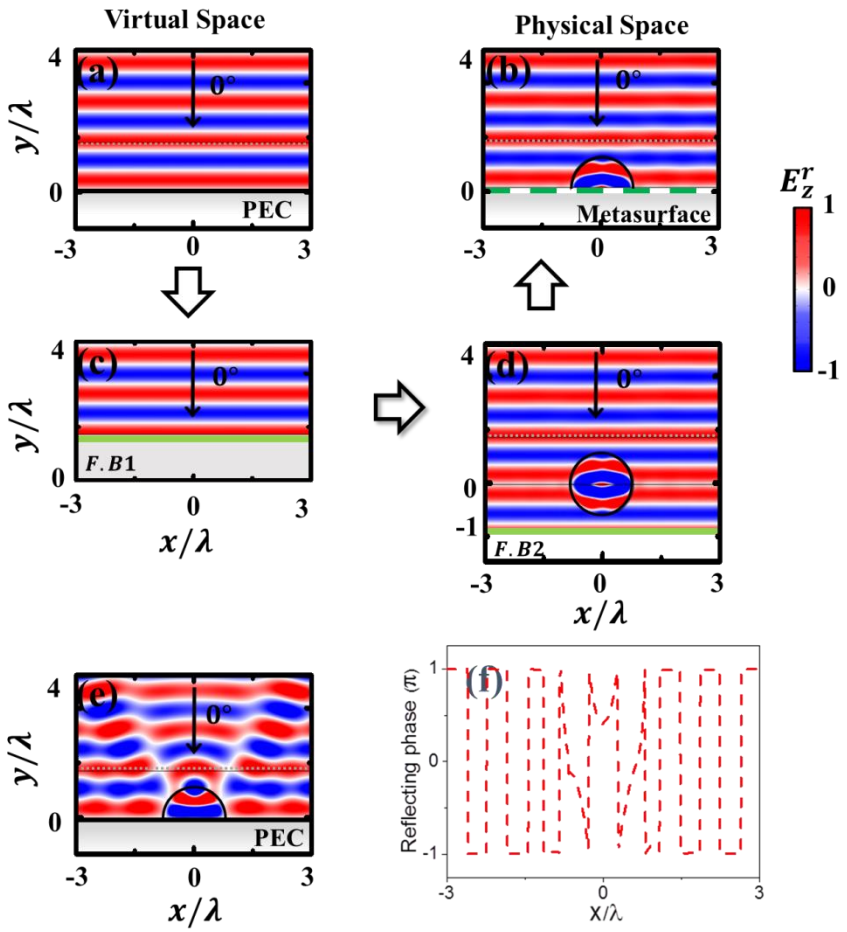

Figure 2. (color online). Simulation results in each step of design procedure of metasurface external cloak. (a) The virtual space with a flat PEC. (b) The physical space with the “real” object. (c, d) are the auxiliary “virtual” spaces. (e) The “real” object with a flat PEC. (f) Required reflecting phase for the metasurface.

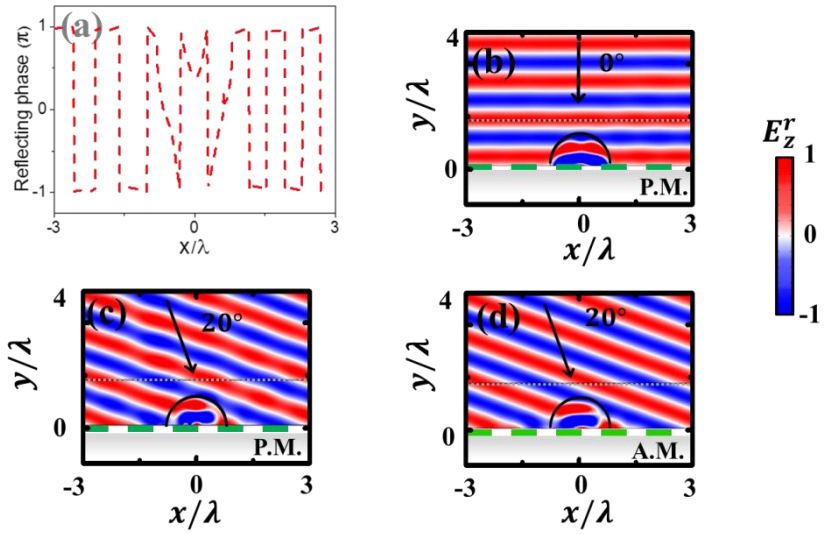

Figure 3. (color online). Angular performance of metasurface external cloak. (a) Required reflection phase profile of metasurface. (b) E_z profile at incidence angle of 0° using a passive metasurface. (c) E_z profile at incidence angle of 20° using a passive metasurface. (d) Corresponding simulation result for the ideal case of an active metasurface.

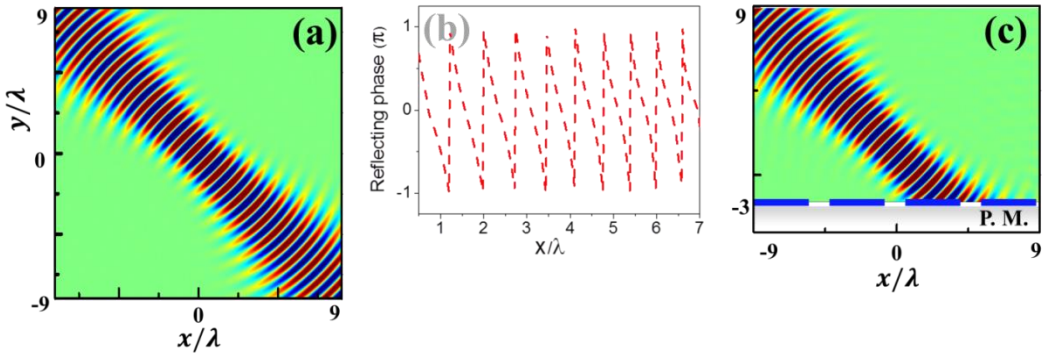

Figure 4. (color online). (a) The target standing wave from two counter-propagating coherent Gauss beams obliquely incident at opposite directions, where the angle of incidence is 45 degrees. (b) Required reflecting phase for the designed metasurface. (c) By replacing a coherent Gauss beam with designed passive metasurface, the same standing wave can be generated with only one Gauss beam.

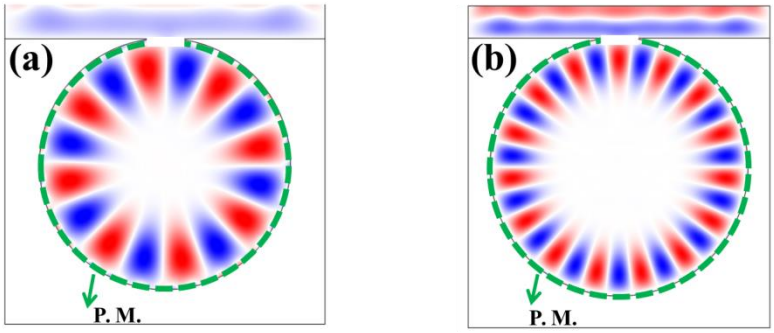

Figure 5. (color online). The cavity modes constructed using passive metasurfaces (the green dashed line), now with simply air as cavity volume instead of dielectric. A plane wave is used to excite the cavity through a small gap at the top. (a) a WGM with order $m = 8$ from a metasurface cavity diameter $d = 8\lambda$. (b) a WGM with order $m = 15$ from a metasurface cavity diameter $d = 13\lambda$.

REFERENCES AND NOTES

1. Yu, N.; Genevet, P.; Kats, M. A.; Aieta, F.; Tetienne, J. P.; Capasso, F.; Gaburro, Z. Light propagation with phase discontinuities: generalized laws of reflection and refraction. *Science*, **2011**, *334*, 333-337.

2. Ni, X.; Emani, N. K.; Kildishev, A. V.; Boltasseva, A.; Shalaev, V. M. Broadband light bending with plasmonic nanoantennas. *Science*, **2012**, *335*, 427-427.

3. Kildishev, A. V.; Boltasseva, A.; Shalaev, V. M. Planar photonics with metasurfaces. *Science*, **2013**, *339*, 1232009.

4. Sun, S.; He, Q.; Xiao, S.; Xu, Q.; Li, X.; Zhou, L. Gradient-index meta-surfaces as a bridge linking propagating waves and surface waves. *Nature Materials*, **2012**, *11*, 426-431.

5. Yu, N.; Capasso, F. Flat optics with designer metasurfaces. *Nature Materials*, **2014**, *13*, 139-150.

6. Aieta, F.; Kats, M. A.; Genevet, P.; Capasso, F. Multiwavelength achromatic metasurfaces by dispersive phase compensation. *Science*, **2015**, *347*, 1342-1345.

7. Lin, D.; Fan, P.; Hasman, E.; Brongersma, M. L. Dielectric gradient metasurface optical elements. *Science*, **2014**, *345*, 298-302.

8. Lin, J.; Mueller, J. B.; Wang, Q.; Yuan, G.; Antoniou, N.; Yuan, X. C.; Capasso, F. Polarization-controlled tunable directional coupling of surface plasmon polaritons. *Science*, **2013**, *340*, 331-334.

9. Genevet, P.; Yu, N.; Aieta, F.; Lin, J.; Kats, M. A.; Blanchard, R.; Capasso, F. Ultra-thin plasmonic optical vortex plate based on phase discontinuities. *Applied Physics Letters*, **2012**, *100*, 013101.

10. Huang, L.; Chen, X.; Mühlenbernd, H.; Zhang, H.; Chen, S.; Bai, B.; Li, J. Three-dimensional optical holography using a plasmonic metasurface. *Nature*

Communications, **2013**, *4*, 3808.

11. Ni, X.; Kildishev, A. V.; Shalaev, V. M. Metasurface holograms for visible light. *Nature communications*, **2013**, *4*, 2807.

12. Zheng, G.; Mühlenbernd, H.; Kenney, M.; Li, G.; Zentgraf, T.; Zhang, S. Metasurface holograms reaching 80% efficiency. *Nature Nanotechnology*, **2015**, *10*, 308-312.

13. Pendry, J. B.; Schurig, D.; Smith, D. R. Controlling electromagnetic fields. *Science*, **2006**, *312*, 1780-1782.

14. Schurig, D.; Mock, J. J.; Justice, B. J.; Cummer, S. A.; Pendry, J. B.; Starr, A. F., Smith, D. R. Metamaterial electromagnetic cloak at microwave frequencies. *Science*, **2006**, *314*, 977-980.

15. Li, J.; Pendry, J. B. Hiding under the carpet: a new strategy for cloaking. *Physical Review Letters*, **2008**, *101*, 203901.

16. Liu, R.; Ji, C.; Mock, J. J.; Chin, J. Y.; Cui, T. J.; Smith, D. R. Broadband ground-plane cloak. *Science*, **2009**, *323*, 366-369.

17. Chen, X.; Luo, Y.; Zhang, J.; Jiang, K.; Pendry, J. B.; Zhang, S. Macroscopic invisibility cloaking of visible light. *Nature Communications*, **2011**, *2*, 176.

18. Zhang, B.; Luo, Y.; Liu, X.; Barbastathis, G. Macroscopic invisibility cloak for visible light. *Physical Review Letters*, **2011**, *106*, 033901.

19. Yang, Y.; Jing, L.; Zheng, B.; Hao, R.; Yin, W.; Li, E.; Chen, H. Full‐Polarization 3D Metasurface Cloak with Preserved Amplitude and Phase. *Advanced Materials*, **2016**, *28*, 6866-6871.

20. Orazbayev, B.; Mohammadi Estakhri, N.; Alù, A.; Beruete, M. Experimental Demonstration of Metasurface‐Based Ultrathin Carpet Cloaks for Millimeter Waves. *Advanced Optical Materials*, **2017**, *5*, 1600606.

21. Ni, X. ; Wong, Z. J.; Mrejen, M.; Wang, Y.; Zhang, X. An ultrathin invisibility skin cloak. *Science*, **2015**, *349*, 1310-1314.

22. Wei, M.; Yang, Q.; Zhang, X.; Li, Y.; Gu, J.; Han, J.; Zhang, W. Ultrathin metasurface-based carpet cloak for terahertz wave. *Optics Express*, **2017**, *25*, 15635-15642.

23. Teperik, T. V.; Burokur, S. N.; de Lustrac, A.; Sabanowski, G.; Piau, G. P. Experimental validation of an ultra-thin metasurface cloak for hiding a metallic obstacle from an antenna radiation at low frequencies. *Applied Physics Letters*, **2017**, *111*, 054105.

24. Teo, J. Y. H.; Wong, L. J.; Molardi, C.; Genevet, P. Controlling electromagnetic fields at boundaries of arbitrary geometries. *Physical Review A*, **2016**, *94*, 023820.

25. Lai, Y.; Chen, H.; Zhang, Z. Q.; Chan, C. T. Complementary media invisibility cloak that cloaks objects at a distance outside the cloaking shell. *Phys. Rev. Lett.*, **2009**, *102*, 093901.

26. Lai, Y.; Ng, J.; Chen, H.; Han, D.; Xiao, J.; Zhang, Z.Q.; Chan, C.T. Illusion optics: the optical transformation of an object into another object. *Phys. Rev. Lett.*, **2009**, *102*, 253902.

27. Lindell, I. V.; Sihvola, A. H. Realization of impedance boundary. *IEEE Transactions on Antennas and Propagation*, **2006**, *54*, 3669-3676.

28. Liu, F.; Xiao, S.; Sihvola, A.; Li, J. Perfect Co-Circular Polarization Reflector: A Class of Reciprocal Perfect Conductors with Total Co-Circular Polarization Reflection. *IEEE Transactions on Antennas and Propagation*, **2014**, *62*, 6274-6281.

29. Wei, P.; Xiao, S.; Xu, Y.; Chen, H.; Chu, S. T.; Li, J. Metasurface-loaded waveguide for transformation optics applications. *Journal of Optics*, **2016**, *18*, 044015.

30. Zemánek, P.; Jonáš, A.; Šrámek, L.; Liška, M. Optical trapping of nanoparticles and microparticles by a Gaussian standing wave. *Optics letters*, **1999**, *24*, 1448-1450.

31. Ashkin, A.; Dziedzic, J. M.; Bjorkholm, J. E.; Chu, S. Observation of a single-beam gradient force optical trap for dielectric particles. *Optics letters*, **1986**, *11*, 288-290.

32. Kim, Y.; Lee, S. Y.; Ryu, J. W.; Kim, I.; Han, J. H.; Tae, H. S.; Min, B. Designing whispering gallery modes via transformation optics. *Nature Photonics*, **2016**, *10*, 647–652.

33. Vollmer, F.; Arnold, S. Whispering-gallery-mode biosensing: label-free detection down to single molecules. *Nature Methods*, **2008**, *5*, 591-596.

ToC Figure

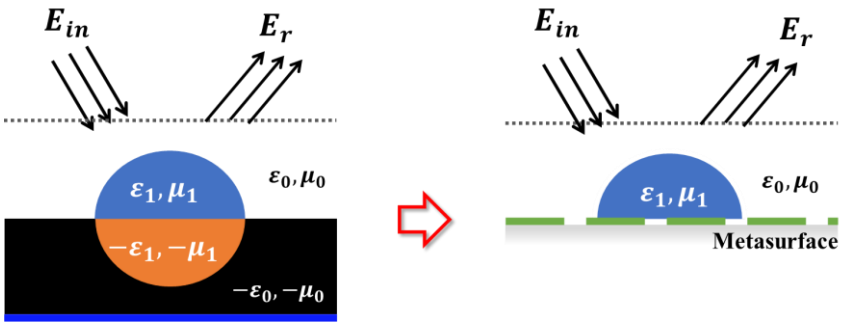

34. Yang, Y.; Jing, L.; Zheng, B.; Hao, R.; Yin, W.; Li, E.; Chen, H. Full‐Polarization 3D Metasurface Cloak with Preserved Amplitude and Phase. *Advanced Materials*, **2016**, *28*, 6866-6871.

35. Orazbayev, B.; Mohammadi Estakhri, N.; Alù, A.; Beruete, M. Experimental Demonstration of Metasurface‐Based Ultrathin Carpet Cloaks for Millimeter Waves. *Advanced Optical Materials*, **2017**, *5*, 1600606.

36. Ni, X. ; Wong, Z. J.; Mrejen, M.; Wang, Y.; Zhang, X. An ultrathin invisibility skin cloak.

Science, **2015**, *349*, 1310-1314.

37. Wei, M.; Yang, Q.; Zhang, X.; Li, Y.; Gu, J.; Han, J.; Zhang, W. Ultrathin metasurface-based carpet cloak for terahertz wave. *Optics Express*, **2017**, *25*, 15635-15642.

38. Teperik, T. V.; Burokur, S. N.; de Lustrac, A.; Sabanowski, G.; Piau, G. P. Experimental validation of an ultra-thin metasurface cloak for hiding a metallic obstacle from an antenna radiation at low frequencies. *Applied Physics Letters*, **2017**, *111*, 054105.